Received: 6 June 2019 | Revised: 3 December 2019 | Accepted: 26 January 2020

DOI: 10.1111/cmi.13179

RESEARCH ARTICLE

WILEY

17-β-Estradiol increases macrophage activity through activation of the G-protein-coupled estrogen receptor and improves the response of female mice to *Cryptococcus gattii*

Marliete C. Costa[1] | Heliana de Barros Fernandes[2] | Gleisy K. N. Gonçalves[3] | Anderson P. N. Santos[1] | Gabriella F. Ferreira[4] | Gustavo J. C. de Freitas[1] | Paulo H. F. do Carmo[1] | Jôsy Hubner[2] | Elúzia C. P. Emídio[1] | Julliana R. A. Santos[6] | Jane L. dos Santos[7] | Adelina M. dos Reis[3] | Caio T. Fagundes[5] | Aristóbolo M. da Silva[2] | Daniel A. Santos[1]

[1]Laboratório de Micologia, Departamento de Microbiologia, ICB-UFMG, Belo Horizonte, Brazil

[2]Laboratório de Genes Inflamatórios, Departamento de Morfologia, ICB-UFMG, Belo Horizonte, Brazil

[3]Laboratório de Endocrinologia e Metabolismo, Departamento de Fisiologia, ICB-UFMG, Belo Horizonte, Brazil

[4]Campus Governador Valadares, Programa Multicêntrico de Pós Graduação em Bioquímica e Biologia Molecular—UFJF, Juiz de Fora, Brazil

[5]Laboratório de Interação Microrganismo-Hospedeiro, Departamento de Microbiologia, ICB-UFMG, Belo Horizonte, Brazil

[6]Laboratório de Microbiologia Ambiental, UniCEUMA, São Luís, Brazil

[7]Laboratório de Imunobiologia, DCB-UESC, Ilhéus, Brazil

Correspondence
Daniel A. Santos, Departamento de Microbiologia, Instituto de Ciências Biológicas, Universidade Federal de Minas Gerais, Av. Antônio Carlos, 6627, PO Box 486, Belo Horizonte 31270-901, MG, Brazil. Tel.: +55 3349 7700;
Fax: +55 31 3409 2758.
Email: das@ufmg.br; dasufmg@gmail.com

Funding information
Conselho Nacional de Desenvolvimento Científico e Tecnológico, Grant/Award Numbers: 403006/2016-3, 440010/2018-7, 302670/2017-3; Coordenação de Aperfeiçoamento de Pessoal de Nível Superior; Fundação de Amparo à Pesquisa do Estado de Minas Gerais, Grant/Award Numbers: APQ-00727-16, PPM-00061-18

Abstract

Cryptococcus gattii (Cg) is one of the agents of cryptococcosis, a severe systemic mycosis with a higher prevalence in men than women, but the influence of the female sex hormone, 17-β-estradiol (E2), on cryptococcosis remains unclear. Our study shows that female mice presented delayed mortality, increased neutrophil recruitment in bronchoalveolar lavage fluid, and reduced fungal load after 24 hr of infection compared to male and ovariectomised female mice (OVX). E2 replacement restored OVX female survival. Female macrophages have more efficient fungicidal activity, which was increased by E2 and reversed by the antagonist of G-protein-coupled oestrogen receptor (GPER), which negatively modulates PI3K activation. Furthermore, E2 induces a reduction in Cg cell diameter, cell charge, and antioxidant peroxidase activity. In conclusion, female mice present improved control of Cg infection, and GPER is important for E2 modulation of the female response.

KEYWORDS

17-β-estradiol, cryptococcosis, *Cryptococcus gattii*, GPER

1 | BACKGROUND

Cryptococcosis is a serious fungal disease worldwide caused by the encapsulated yeast *Cryptococcus* spp. The main agents, *Cryptococcus gattii* (Cg) and *Cryptococcus neoformans*, are transmitted by inhalation and reach the inferior respiratory tract, which results in pneumonia. Within the lungs, fungal cells can be taken up by phagocytes and translocated from the respiratory site to the central nervous system, resulting in meningoencephalitis (Charlier et al., 2008; Mora et al., 2015; Santiago-Tirado, Onken, Cooper, Klein, & Doering, 2017). Globally, cryptococcal meningitis was responsible for 15% of AIDS-related deaths in 2014 (181.100 deaths; Rajasingham et al., 2017). In a most recent large series of autopsies carried out in the low-income countries, Mozambique and Brazil, over 40% of patients with cryptococcosis were immunocompetent (Hurtado et al., 2019). Among non-HIV-infected patients in Latin America, *C. gattii* VGII is reported as the main agent; in both HIV-infected and non-infected populations, most cases of cryptococcosis are reported in young males (Firacative, Lizarazo, Illnait-Zaragozí, Castañeda, & Latin American Cryptococcal Study Group, 2018; Shaheen, Somayaji, Myers, & Mody, 2018).

Like many diseases (Clemons, Shankar, & Stevens, 2016), fungal infections caused by *Paracoccidioides brasiliensis* (Shankar, Restrepo, Clemons, & Stevens, 2011) and *Candida albicans* (Fidel, Cutright, & Steele, 2000) are also influenced by sex and female hormones. There are strong differences between the sexes in immunity to infection, suggesting that sex hormones modulate the immune response; for example, estrogen receptors (ERs) regulate cellular activities and pathways in the innate and adaptive immune system, as well as modifying immune cell development (Kovats, 2015). The predominant form of estrogen, 17-β-estradiol (E2), is the major female sex hormone and is characterised by a high affinity for two major ER subtypes, ER-α and ER-β (Campesi, Marino, Montella, Pais, & Franconi, 2017; Kovats, 2015). It is also associated with a recently characterised G-protein-coupled oestrogen receptor (GPER; Pupo, Maggiolini, & Musti, 2016). Their classic actions involve transcriptional regulation of a large number of genes; however, membrane-associated ER effects are now widely characterised, but the direct effects of the activation of ERs on the innate immune response to a fungal infection have not been thoroughly evaluated (Kovats, 2015; Pupo et al., 2016). Indeed, the specific mechanisms responsible for this sex-based disparity in cryptococcosis are still unknown. In this sense, the goal of this study was to understand the mechanisms of host responses to Cg generated by female sex hormones. We used a hormone-manipulated murine model of Cg infection to test the impact of E2 on survival and fungal clearance, with a particular focus on the impact of the different ERs on macrophage responses to the fungus. Lastly, we determined the influence of E2 on the morphophysiology of the fungi. Our results reinforce the importance of E2 in the female response against Cg.

2 | RESULTS

2.1 | Mortality and fungal load are higher in male mice 24 hr post infection, removal of gonads eliminates sex differences during Cg infection, and E2 re-establishes survival of OVX mice

To study the influence of sex on susceptibility to Cg infection, male and female mice were compared with respect to survival after infection with Cg. Death occurred earlier in males than in females ($p < .05$; Figure 1a). Death events began on Day 13 in males and on Day 22 in females. Whereas only 40% of female animals had succumbed at Day 32, all males had already succumbed. In order to verify if gonadal hormones are determinants of this response, we performed a gonadectomy in both sexes. The removal of the gonads eliminates the sexual dimorphism associated with the survival of animals with cryptococcosis (Figure 1a). When comparing Sham and OVX females, it was observed that removal of the main source of female hormones significantly reduced ($p < .05$) survival; 80% of OVX females had succumbed, whereas the mortality rate was 40% in normal females at 24 days. Gonad removal did not alter survival in male mice (Figure 1a). Given the ovaries' impact on female Cg infection, E2 replacement with 100 ug of E2 was performed in female mice. When infected with Cg, the OVX females receiving E2 (OVX + E2) survived similarly to normal females (Figure 1a), but hormonal replacement did not significantly alter the fungal burden recovery from OVX + E2 mice. Ovariectomy caused a marked decrease in uterine weight, and the uterine involution was significantly reverted by E2 injection (Figure 1b), confirming the success of the protocol. In an earlier stage of infection, 24 hr, Cg was not detected in the brains of mice from either sex. There was no difference in lung CFU, but the BALF of female mice presented a reduced fungal load compared with that of male mice ($p < .05$; Figure 1c). The fungal burden in BALF from gonadectomised animals increased significantly ($p < .05$), reducing sex differences; however, only ovariectomy increases CFU recovery from the lungs ($p < .05$; Figure 1c,d). Although E2 does not mitigate the OVX phenotype, there was a reduction of approximately 30% and 40% of CFU in the lungs and BALF, respectively, of OVX + E2 compared with untreated OVX females after 24 hr of infection (Figure 1d). When we analysed the fungal burden in organs from male and female mice at Day 15, there was no difference in fungal burden in the brain, lungs, and BALF (Figure 1e). However, male mice have increased brain transmigration, with 100% presenting Cg detection, whereas female mice were 70% positive for the presence of fungi (data not shown).

2.2 | Neutrophil recruitment in Cg infection is regulated by E2

To better understand the male and female response to Cg infection, we performed cell phenotyping of BALF to characterise the neutrophil and macrophage involvement in initial immune response (the gating

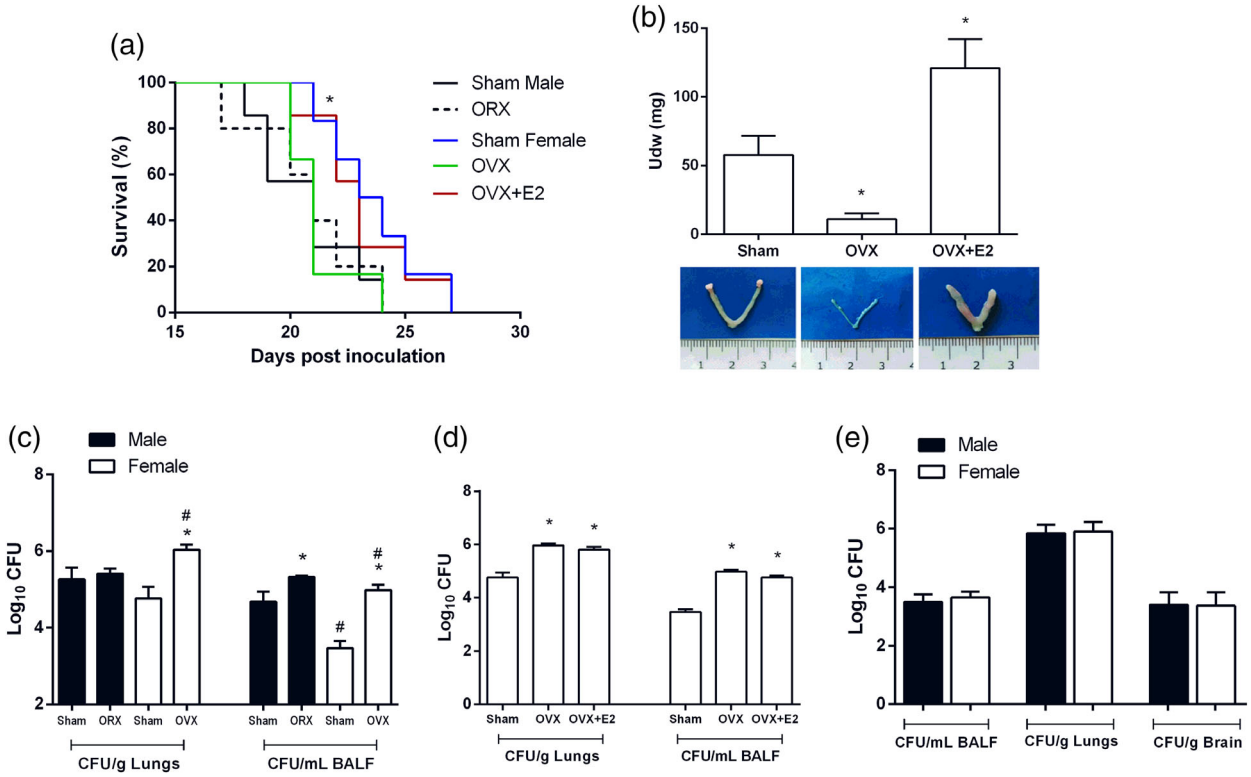

FIGURE 1 Cg infection causes earlier mortality in male than female mice, and E2 influences female survival during Cg infection. Male mice were orchiectomised (OVX) and female mice were ovariectomised and/or received 100 μg of E2 post gonad removal. Sham male, sham female, male ORX, female OVX, and female OVX + E2 infected with 1×10^5 of Cg, and survival rates were obtained ($n = 6$). Results are presented as percent survival post infection (a). From female mice, uterus weights were obtained (Udw) to confirm uterotrophic activity after ovariectomy and hormonal reconstitution (b). The photos below graphic B are representative of one female mouse per group. Twenty-four hours after infection, mouse groups were euthanised to determine the impact of gonadectomy on sex, CFU recovery from the lungs and BALF (c) and for analyses of E2, the influence on female CFU load on the same organs was determined (d). At a later time, 15 days after infection, BALF, lungs, and brains of male and female mice were obtained to check disease progression by fungal burden (e). The bars represent the mean ± *SD*, and the results were expressed as CFU per millilitre of BALF and per gram of the lungs. $^*p$ were significantly different ($p < .05$) related to respective Sham from same sex. $^\#p$ were significantly different ($p < .05$) related to the opposite sex from the same profile (Sham male × Sham female; ORX male × OVX female). BALF, bronchoalveolar lavage fluid

strategy is available in Figure S1). Males and OVX females presented a higher rate of recruitment of total leukocytes related to normal and OVX + E2 females ($p < .05$; Figure 2a). Normal females and OVX + E2 presented an intense neutrophil recruitment in BALF ($p < .05$; Figure 2b). Also, ovarian removal directly reduced the amount of these cells. There was no marked difference in the number of macrophage populations, which were analysed according to the level of CD11c expression: low level, interstitial macrophages (Figure 2c); high level, alveolar macrophages (Figure 2d). Indeed, we also observed decreased levels of CXCL-1 in BALF from OVX mice ($p < .05$; Figure 2e).

2.3 | E2 improves internalisation and fungicidal activity of female mouse macrophages

Although there were no differences in macrophage recruitment in BALF, we questioned if these cells have altered activity in the presence of E2. The percentage of mature macrophages obtained from the BMDM protocol averaged 95% to 99%, and no additional purification was required (Figure S2). Improved phagocytosis (PI) by female BMDM was observed both 2 and 24 hr after Cg infection (Figure 3a), and E2 improved this activity. E2 upregulated the expression of TLR-2, but not of TLR4 and dectin-1 in BMDM in comparison with non-infected (NI) BMDM (Figure 3b). A reduced fungal burden inside macrophages ($p < .05$) from females was observed in comparison with male BMDMs, and E2 was able to increase killing activity, leading to a reduced fungal burden inside female cells (Figure 3c). Male BMDMs were not influenced by E2. BMDMs from females produced higher amounts of ROS ($p < .05$), expressed as arbitrary units (AU) of fluorescence, and E2 increased this effect ($p < .05$; Figure 3d).

2.4 | E2 improves BMDM activity against Cg through GPER signalling in females

In view of the influence of E2 on the activity of BMDMs in females, we first decided to evaluate their mRNA levels of the E2 receptors ER-α, ER-β, and GPER. Initially, we verified that the levels of ER-α and

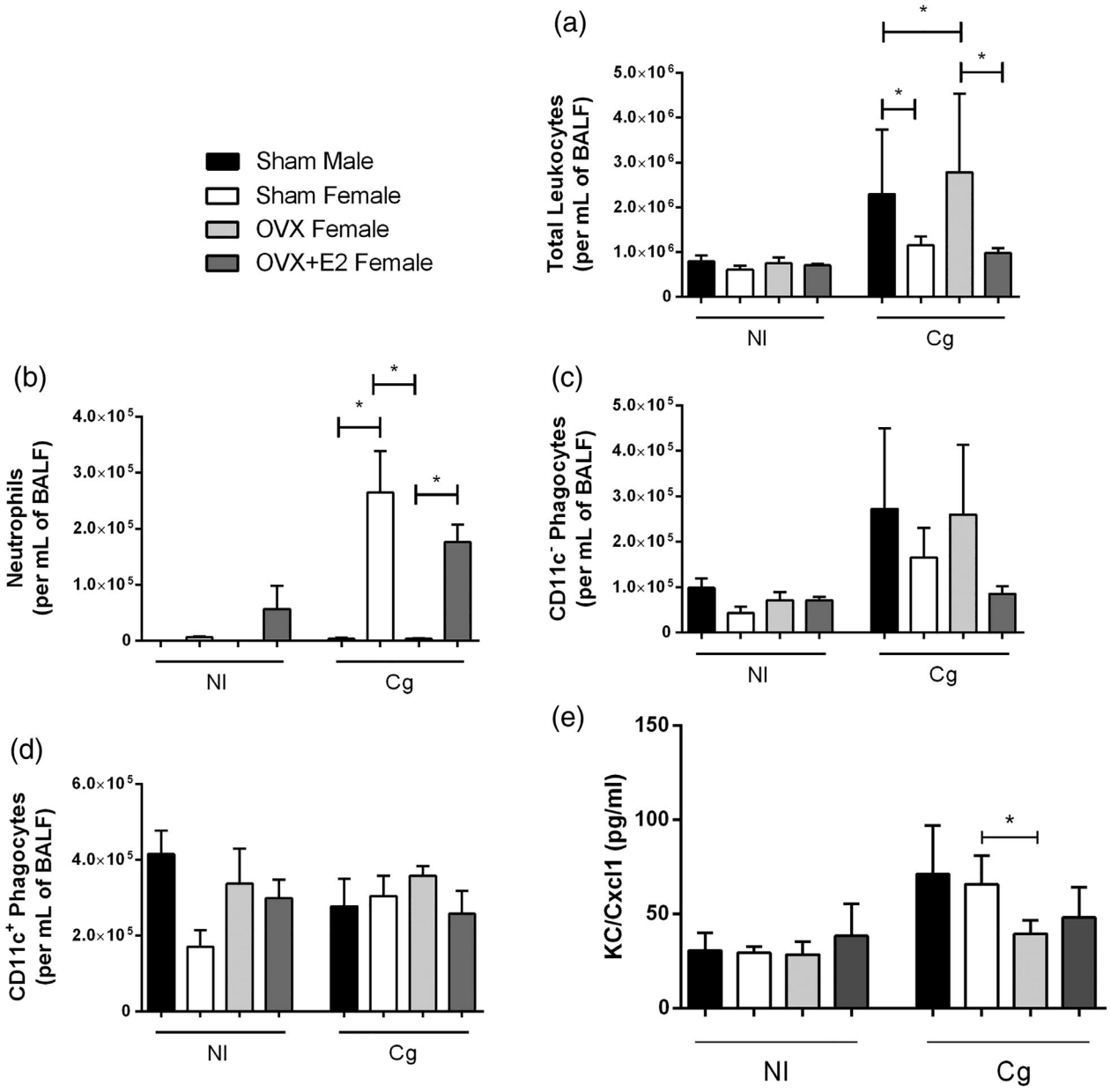

FIGURE 2 E2 induces neutrophilic recruitment in the setting of Cg infection. Groups (n = 5) of nongonadectomised males and females, ovariectomised (OVX), and ovariectomised females with E2 treatment (OVX + E2) were infected with Cg, and 4 day after inoculation, (a) total leukocytes in BALF were obtained for flow cytometry analyses for the presence of (b) neutrophils, (c) $CD11c^{-}$, and (d) $CD11c^{+}$ cells. Supernatants were used for the quantification of (e) CXCL1. The bars represent the mean ± *SD*, and the results were expressed as cell counts per millilitre of BALF, and CXCL1 is expressed in picograms per millilitre of BALF. *p were significantly different ($p < .05$). NI, non-infected; OVX, ovariectomised female; OVX + E2, ovariectomised female with E2

GPER transcripts were more abundant (Figure 4a). Because the mRNA levels of ER-β were almost undetectable (Figure 4a), we decided to focus on the signalling pathway triggered by ER-α and GPER. Using specific antagonists to these receptors, we observed that ER-α and GPER blockage (by TPBM and G15, respectively) reduced the PI (Figure 4b; $p < .05$) and impaired the killing activity of macrophages, as evidenced by higher fungal recovery (Figure 4c). We subsequently assayed the dose effect of a GPER agonist (G1) and two GPER antagonists (G15 and G36). G1 was efficient at increasing fungal killing by female BMDMs as well as E2 ($p < .05$). Both antagonists, especially G36, subverted the E2 effect, leading to increased fungal growth inside BMDM ($p < .05$; Figure 4d).

To verify if PI3K/AKT signalling is modulated by GPER in female Cg-infected macrophages, we evaluated its phosphorylation in BMDMs exposed to G1, G15, and G36. The level of phosphorylated PI3K, an activator of AKT, was decreased in male mice upon infection, but it was increased in BMDMs of infected females ($p < .05$). Also, BMDMs of infected females presented higher PI3K activation

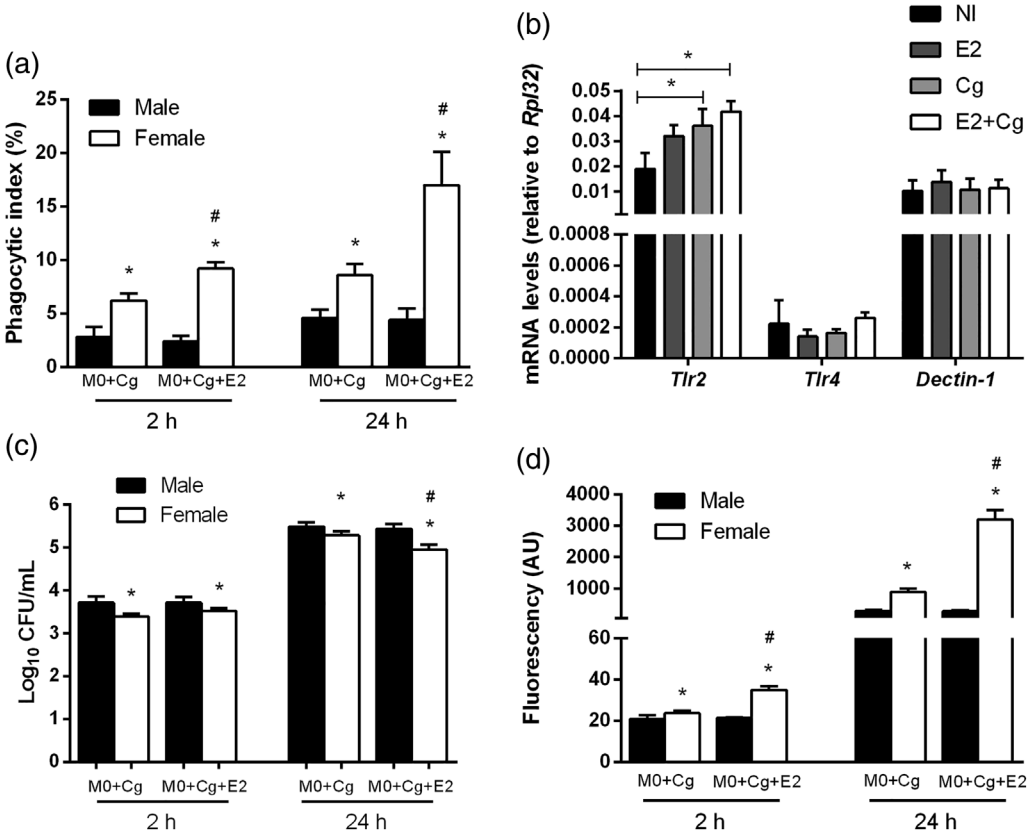

FIGURE 3 Macrophages from female mice have more efficient internalisation and fungicidal activities than those from male mice, and E2 improves this phenotype. Bone marrow-derived macrophages (BMDMs) were treated with E2 and infected with Cg for quantification of (a) phagocytic index; (b) expression of receptors TLR2, TLR4, and dectin-1; (c) killing activity; and (d) ROS production 2 and 24 hr post infection for cells with or without treatment of 10 nM of E2. The bars represent the mean ± *SD*. $^{*}p$ were significantly different ($p < .05$) for the same treatments in BMDMs of the opposite sex. $^{\#}p$ were significantly different ($p < .05$) from untreated controls. NI, non-infected; M0 + Cg, macrophage infected; M0 + Cg + E2, macrophage treated with E2, then infected

than those of infected males. Also, G36 reduced PI3K phosphorylation in Cg and non-infected cells (Figure 5a). Female macrophages presented increased basal AKT activity, even without infection (Figure 5b; $p < .05$). After Cg infection, AKT phosphorylation was not altered in female BMDM). These effects were dependent on E2, because AKT phosphorylation was reduced when GPER antagonists (G15 or G36) were used. Although treatment with G1 in infected cells led to lower phosphorylation of AKT, treatment with E2 was effective and maintained high AKT activity (Figure 5b). Infected BMDMs from males have reduced expression of catalase (Figure 5c) and increased expression of gp91 (NADPH; Figure 5d), whereas BMDMs from females were not observed to alter phosphorylation of these proteins.

2.5 | E2 induces important physiological modifications in Cg

The yeast diameter was significantly lower ($p < .05$) in the presence of E2 (Figure 6a), and there was no alteration in the capsule size (Figure 6b). However, E2 reduced the ZP (Figure 6c). Analysis of TBARS (Figure 6d) and ROS levels in the presence of HP (Figure 6e) demonstrated that cells grown in the presence of E2 are more susceptible to oxidative stress induced by hydrogen peroxide than cells grown without the hormone ($p < .05$). These results were corroborated for PER enzyme activity (Figure 6f) data (but not SOD activity, Figure 6g), because the activity of the peroxidase enzyme is reduced in the presence of E2 ($p < .05$). Further, in the antifungal susceptibility testing, the MICs of AMB and HP were 0.5 and 136 mg L^{-1}, respectively. In the presence of 10-nM E2, these values were reduced to 0.06 mg L^{-1} for AMB and 64 mg L^{-1} for HP.

3 | DISCUSSION

The first studies that aimed to clarify the influence of sex hormones on cryptococcosis were published in 2002 and 2013, but little is known about the mechanisms of this influence (Lortholary, Improvisi, Fitting, Cavaillon, & Dromer, 2002; McClelland et al., 2013). Our study using a murine model of pulmonary infection by Cg demonstrated that male mice are more susceptible to Cg, presenting earlier death events than females, higher fungal loads in BALF at 24 after infection and

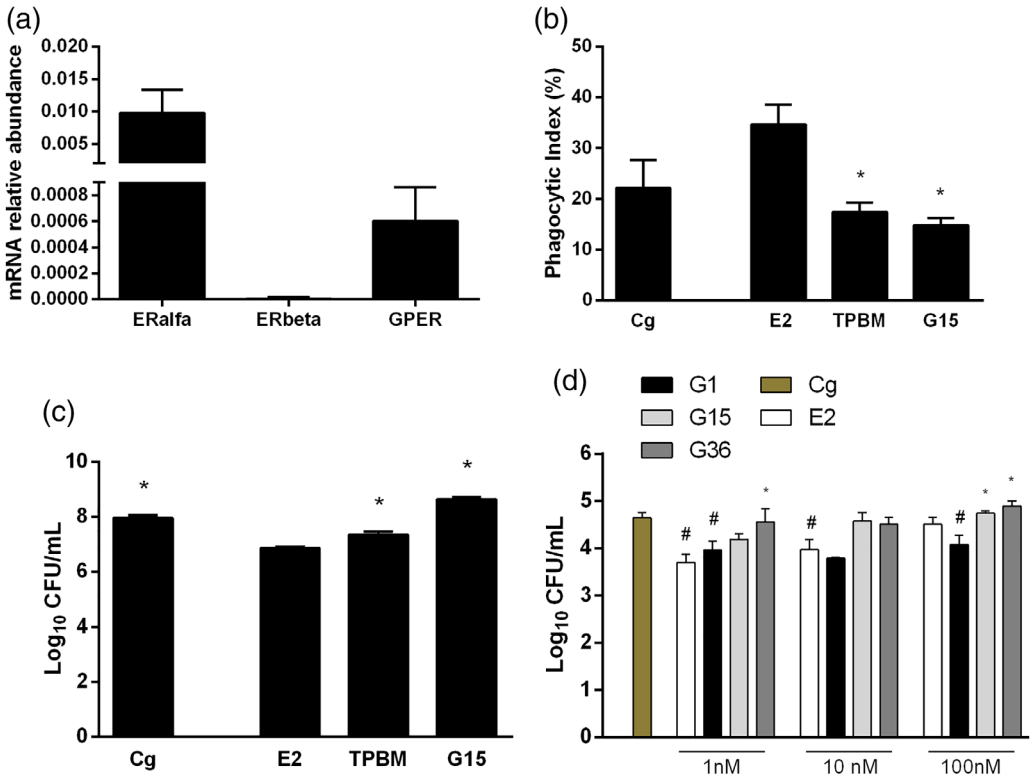

FIGURE 4 E2 improves the activity of female cells against Cg through GPER. Bone marrow-derived macrophages from females were obtained for the determination of (a) the relative abundance of estrogen receptors (ER) alpha, ER beta, and GPER; (b) phagocytic index; and (c) the killing activity 24 hr after infection in the presence of 10-nM TPBM and G15 (oestrogen receptor antagonists of ER-α and GPER, respectively). After that, (d) the impact of GPER modulation on killing activity 24 hr after infection was evaluated using 1, 10, or 100 nM of the agonist, G1 and the antagonists, G15, and G36. Bars represent the mean ± *SD*. **p* were significantly different ($p < .05$) compared with E2. #*p* were significantly different ($p < .05$) compared with Cg. Cg, Cg-infected macrophages; E2, macrophage treated with E2 then infected; TPBM, G15, G1, and G36, macrophage treated with these molecules, then treated with E2, and then infected. TPBM, theophylline, 8-[(benzylthio)methyl]. G1: (±)-1-[(3aR*,4S*,9bS*)-4-(6-Bromo-1,3-benzodioxol-5-yl)-3a,4,5,9b-tetrahydro-3*H*-cyclopenta[*c*]quinolin-8-yl]-ethenone. G15: (3aS*,4R*,9bR*)-4-(6-Bromo-1,3-benzodioxol-5-yl)-3a,4,5,9b-3*H*-cyclopenta[*c*]quinoline. G36: (±)-(3aR*,4S*,9bS*)-4-(6-Bromo-1,3-benzodioxol-5-yl)-3a,4,5,9b-tetrahydro-8-(1-methylethyl)-3*H*-cyclopenta[*c*]quinoline

increased brain transmigration, with 100% presenting Cg detection 15 days post infection. To investigate the role of sex-dominant hormones in cryptococcosis, the primary source of testosterone and E2, testicles, and ovaries, respectively, were removed. Only ovariectomy (not orchiectomy) influences the survival rate, and this was attenuated by timely E2 replacement. This confirmed that this hormone positively coordinates the female response to Cg. Furthermore, previous studies have demonstrated that testosterone has multiple depressive effects on the immune system (McClelland et al., 2013; Pennell, Galligan, & Fish, 2012; Pinzan, Ruas, Casabona-Fortunato, Carvalho, & Roque-Barreira, 2010). These results support epidemiological data that indicate the higher occurrence rate of this disease in males (Firacative et al., 2018; Shaheen et al., 2018).

Lortholary et al. (2002) were the first to demonstrate—in a murine model of intravenous infection—that sex may influence the polarisation of the immune response in males and females infected with *C. neoformans*, which served as the model for our study with Cg. Upon entering the lungs, Cg cells are recognised by host innate immune cells that are responsible for ingesting and destroying invading pathogens, presenting antigens to T cells, and producing mediators (cytokines and chemokines) that initiate and direct the adaptive immune response. Depletion of neutrophil, resident pulmonary DCs, and alveolar macrophages results in rapid deterioration and death of mice infected with *Cryptococcus* (Osterholzer et al., 2009). These cells link the innate and adaptive immune systems during *Cryptococcus* infection. For example, during human infection, T-cell percentages in both males and females dropped significantly compared with uninfected controls. However, as shown in previous studies, even though male PBMCs were proliferating in response to infection, all measured T-cell markers were significantly lower in males than females in infected groups, suggesting a weakened T-cell response in males in the presence of *C. neoformans* (Guess, Rosen, Castro-Lopez, Wormley, & McClelland, 2019). This difference certainly begins in the early moments of infection, with differences in counts and activities of innate cells, leading to a more effective late response in women.

Neutrophils are involved in the early stages of immune responses to pathogens. In the early stages of infection, they are the most abundant cells, and they determine the clearance of the fungus by

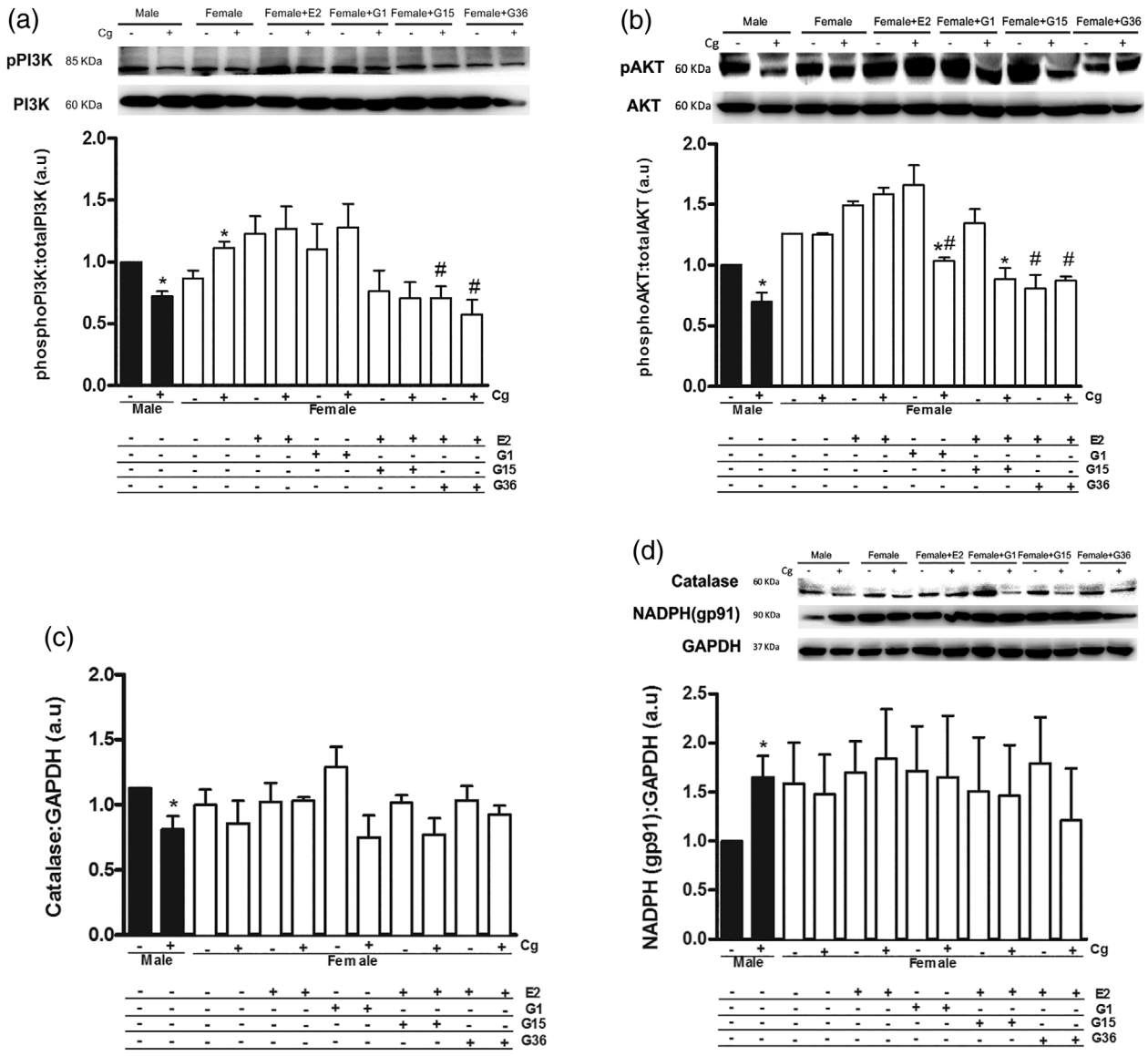

FIGURE 5 Macrophages from female mice have a more efficient intracellular response against Cg. Protein expression of bone marrow-derived macrophages from male and female mice were evaluated by western blot directed against (a) pPI3K, (b) p-AKT, (c) gp91(NADPH), and (d) catalase expression 24 hr after infection of cells treated with E2, G1, G15, or G36 (10 nM). Bars represent the mean ± *SD*. **p* were significantly different ($p < .05$) related to the respective non-infected mice. $^{\#}p$ were significantly different ($p < .05$) related to infected and non-infected E2-treated groups. Cg–, non-infected; Cg+, infected

phagocytosis and the release of a myriad of antimicrobial molecules and ROS (Leopold Wager, Hole, Wozniak, & Wormley, 2016; Rocha et al., 2015). Extrapulmonary dissemination of *Cryptococcus* is one of the most critical steps in the development of meningoencephalitis, the fungal burden in the lung parenchyma, and alveolar space (BALF) being determinant factors for the amount of yeast that gain entry to blood vessels. After activation, neutrophils traffic from the vasculature via transendothelial migration through the brain vasculature and lung interstitium and into the alveolar space (Pechous, 2017). Interestingly, the efficiency of the intravascular clearance in the brain is not as great as that in the lung, but the lower efficiency of fungal clearance in the brain vasculature correlates with less efficient recruitment of neutrophils (Sun et al., 2016; Sun & Shi, 2016). In our study, we detected that female mice have increased neutrophil recruitment, and gonadectomy depletes its recruitment to the bronchoalveolar space.

Nevertheless, macrophages are essential for the control of cryptococcosis, as their depletion had a catastrophic effect on any restriction of fungal burden, even when neutrophil numbers were unaffected. Macrophages play a critical role in cryptococcosis progression and outcome, in such a way that macrophages kill cryptococcal cells, or disseminate infection to the brain (Alanio, Desnos-Ollivier, & Dromer, 2011). Although there were no observed differences in the expression (except for TLR2) of receptors for the fungus, BMDMs from females possess increased fungicidal activity compared with male BMDMs. Normal females and OVX + E2 females presented

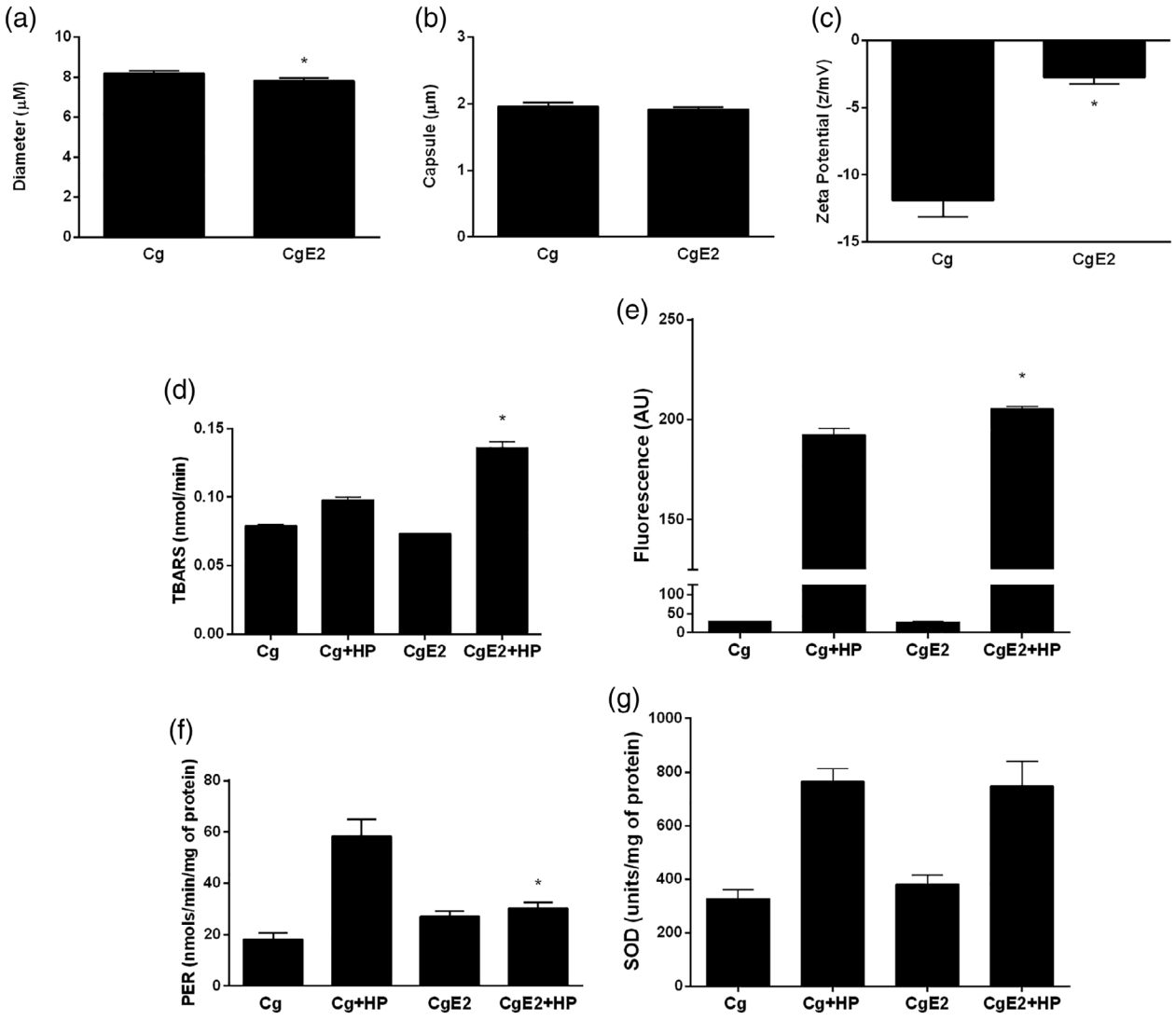

FIGURE 6 E2 induces important physiological modifications in Cg. Cg was grown in the presence or absence of E2, and (a) cell diameter, (b) capsule size, (c) zeta potential, (d) lipid peroxidation, (e) ROS production, (f) PER activity, and (g) SOD activity were measured. Bars represent the mean ± *SD*. **p* were significantly different ($p < .05$). Cg, only Cg; Cg + E2, Cg treated with E2; Cg + HP, Cg treated with hydrogen peroxide; Cg + E2 + HP, Cg treated with E2 and hydrogen peroxide. HP, hydrogen peroxide; PER, peroxidase; SOD, superoxide dismutase; TBARS, thiobarbituric acid-reactive substances

significant reductions in the fungal load in the alveolar space; it is possible that, in addition to higher neutrophilic recruitment, E2 also leads to the augmented activation of macrophages. McClelland et al. (2013) demonstrated that macrophages from females engulfed more *C. neoformans* than macrophages from males, which also presented with higher fungal burdens. Our approach also confirms that Cg replicates more readily in a male environment and that E2 inhibits fungal proliferation (Guess et al., 2019; Lortholary et al., 2002; McClelland et al., 2013). These data are consistent with our results that pointed to the differential interaction between Cg and macrophages within different sex environments. Our study also improves the knowledge in this area, pointing that E2 upregulates TLR2 expression and is fundamental to internalisation, killing, and ROS production by female BMDMs during Cg infection.

There are two major ER subtypes, ER-α and ER-β, and their classic actions are genomic; however, nongenomic and membrane-associated ERs, such as GPER, are now widely recognised (Kovats, 2015; Tica et al., 2016). Using specific antagonists, we revealed that GPER is the target receptor activated by E2 in the Cg-infected BMDMs, although its expression is reduced compared with ER-α. To explore the downstream signalling pathway of the GPER in BMDM, we examined whether PI3K signalling is involved. The various members of the PI3K signalling pathway play several multifaceted roles in macrophage activation. Studies indicate that PI3K contributes to phagosome maturation and regulates NADPH oxidase and catalase activation during phagocytosis (Jang et al., 2004; Quinn & Gauss, 2004). Our data revealed that the P-PI3K ratio was significantly higher in BMDMs from females than in those from males, and the

role of E2 on its activation was confirmed when the GPER antagonist was tested. Although the same was not observed for P-AKT/AKT, basal AKT expression in females is higher than that in BMBMs from males, suggesting a superior immune response in females and indicating the potential for different signalling outputs downstream of PI3K, which is therefore an interesting finding that should be evaluated further. For example, PI3Ks can regulate members of the Rac, Ras, and Arf families of GTPases through the regulation of their GEFs and GAPs (Jimenez, Hernandez, Pimentel, & Carrera, 2002; Pacold et al., 2000). Our data provide novel information about E2 affecting the macrophage Cg response, which turns out to be mediated by GPER signalling.

Furthermore, we considered that Cg may modulate its physiological fitness to adapt to host conditions and cause infection (Ferreira et al., 2015; García-Rodas, Casadevall, Rodríguez-Tudela, Cuenca-Estrella, & Zaragoza, 2011; Nosanchuk et al., 1999; Zaragoza et al., 2008). Our data demonstrated that E2 negatively modulates the physical and physiological activity of Cg. The reduction in cell size observed for cells grown with E2 may not be sufficient to increase Cg ingestion by BMDM, and the reduced ZP is able to reduce the chances of the pathogen establishing cellular infection and dissemination by the Trojan horse mechanism (Nosanchuk et al., 1999). However, in view of the higher phagocytic activity and ROS production by BMDMs from females, we suppose that yeast is more susceptible to phagolysosomes, because there was a reduced fungal activity of peroxidase and higher lipid peroxidation in the presence of hydrogen peroxide and E2. Interestingly, Mohr, Tatem, Long, Muchmore, and Felton (1973) observed that estrogen, but not testosterone, completely suppressed the growth of four isolates of *C. neoformans* at subinhibitory concentrations of Amphotericin B, a drug that causes oxidative burst in cells. In this work, we observed a reduced MIC of AmB and HP in the presence of E2. It is plausible that changes in fungal physiology induced by the presence of E2, together with the greater activity of female macrophages mediated by the GPER, may reflect the higher survival rate observed in Cg-infected females.

In conclusion, our study demonstrates interesting differences in survival induced by sex in Cg infection, clarifying how E2 and other sex-related components may influence cryptococcosis.

4 | EXPERIMENTAL PROCEDURES

4.1 | Mice and ethical statements

Male and female 6-week-old C57BL/6 mice were used for all studies. Animal protocols were approved by the Comissão de Ética no Uso de Animais of Universidade Federal de Minas Gerais (CEUA-UFMG, protocol 34/2016), and all animal experiments were performed according to the guidelines of Brazilian Federal Law 11.794. Mice received food and water ad libitum in a controlled environment with a 12/12 hr light/dark cycle at 23°C. All efforts were made to minimise animal suffering. Any mice that appeared moribund were immediately and humanely euthanised by experienced animal handlers (by cervical dislocation under anaesthesia; ketamine [80 mg kg^{-1}] and xylazine [15 mg kg^{-1}]).

4.2 | Fungal culture

The *C. gattii* (Cg) strain L27/01 used in this study was deposited in the Culture Collection of Microorganisms and Cells of the Universidade Federal de Minas Gerais (UFMG-CM-Y6141; Belo Horizonte, Brazil). The yeast was grown on Sabouraud Dextrose Agar (SDA-KASVI) at 37°C for 48 hr prior to all tests. For mouse experiments, live Cg cells were taken directly from agar plates, washed twice in sterile saline, suspended, and counted for inoculum preparation with a haemocytometer using trypan blue staining to determine the percentage of live cells (which was always higher than 98%). Inocula were normalised to 3.3×10^6 ml^{-1} of live cells for a final inoculum of 30 μl containing 1×10^5 live cells.

4.3 | Experimental design

To understand the influence of sex on the pathogenesis of Cg, **(a)** we first evaluated survival and colony forming units (CFUs) in the lung parenchyma and bronchoalveolar lavage fluid (BALF, alveolar space) of male and female Cg-infected mice. **(b)** Next, to investigate hormonal influences on cryptococcosis, male and female mice were subjected or not to gonadectomy and/or hormonal replacement with E2, then infected with Cg for survival determination, CFU quantification, enzyme-linked immunosorbent assay (ELISA), and flow cytometry in BALF. **(c)** To analyse how sex influences phagocytic activity, bone marrow-derived macrophages (BMDMs) were infected with Cg for phagocytosis, cytotoxicity, and reactive oxygen species (ROS) production assays and quantification of the expression of E2 receptors. **(d)** To reveal the impact of GPER on phagocytic activity in females, female BMDM were infected after stimulation with a specific agonist (G1) or antagonists (G15 and G36) to determine killing and intracellular signalling (chemical names are in the legend of Figure 4). **(e)** Furthermore, Cg was grown in E2-supplemented medium to identify morphological and physiological alterations in yeast cells.

4.4 | Gonadectomy and hormonal replacement

Prior to Cg infection, groups of male and female mice (n = 6) were gonadectomised. Prior to surgery, animals were anaesthetised by intraperitoneal injection of ketamine (80 mg kg^{-1}) and xylazine (15 mg kg^{-1}). Then, males were bilaterally orchiectomised, and females were ovariectomised (OVX; Blakemore & Naftolin, 2016; Zhao, Tian, Hao, & Chen, 2005). The control groups (Sham; n = 6) were submitted to the same surgical procedure except for gonad removal. All animals were given 4 weeks to recover and for their hormonal levels to decrease prior to infection. Furthermore, a group of OVX mice (n = 6) were submitted to hormonal reconstitution through intraperitoneal injection of 100-μg E2 (OVX + E2; Sigma-Aldrich, cat. n. E2758) three times every 48 hr prior to infection, and the injections continued during the entire

experiment. In these same animals, we determined the uterine dry weight (Udw) to evaluate the uterotrophic activity of estradiol in female mice (Sham, OVX and OVX + E2; Blakemore & Naftolin, 2016; Finan et al., 2012; Levin-Allerhand, Sokol, & Smith, 2003).

4.5 | Infection, survival, and determination of fungal burden

Sham, gonadectomised, and OVX + E2 mice were infected with Cg. For intratracheal (i.t.) inoculation, mice were anaesthetised and infected with 30 μl of a suspension containing 10^5 viable Cg cells (Costa et al., 2016; Santos, Holanda, Frases, & Bravim, 2014). For survival analyses, animals (n = 6) were infected and monitored daily, and data are presented as Kaplan–Meier survival curves. After survival studies, two other mouse groups (Sham, gonadectomised, and OVX + E2; n = 6), were infected and euthanised 1 or 15 days after inoculation for fungal burden determination in the brain, lungs, and BALF (data expressed as CFU per gram of organ or CFU per millilitre of BALF). BALF was obtained by surgically exposing the trachea and inserting a plastic catheter (21 gauge). Lavage was performed by slowly injecting 1 ml of cold PBS into the lungs, and fluid was withdrawn three times and kept on ice. The brain and lungs were collected, homogenised in sterile PBS, plated onto SDA, and incubated for 48 hr at 37°C to determine the fungal burden (Costa et al., 2016). The data presented are representative of two independent survival curves, and fungal burdens are representative of two independent experiments.

4.6 | Flow cytometry and ELISA

In addition to survival studies, Sham, OVX, and OVX + E2 (n = 5) mice were infected with 10^5 viable Cg i.t., and BALF was recovered and used for cell phenotype characterisation and CXCL-1 quantification (except for orchiectomised mice; Costa et al., 2016). Cells obtained from BALF were counted, and 1×10^6 cells were fixed and stained to identify non-resident macrophages, marked by F4/80$^+$CD11c$^-$CD11b$^+$, alveolar macrophages represented by the F4/80$^+$CD11c$^+$CD11b$^-$ population and Ly6G$^+$ neutrophils. All conjugated antibodies were purchased from BD Pharmingen. Propidium iodide (PI) staining solution was used to label dead cells (BD Biosciences, San Jose, CA). Compensation was performed using single-colour controls of uninfected animals. Cells were suspended in flow cytometry wash buffer (FWB-R&D System, USA) and analysed with a FACSCantoII (Becton Dickinson, San Diego, CA). Data were analysed with FlowJo software (Treestar, Ashland, OR). Further, the concentration of CXCL1/KC was measured by ELISA with antibody pairs purchased from R&D Systems (R&D Systems, USA) according to the manufacturer's protocol. Results are representative of two independent experiments.

4.7 | Cell culture

BMDMs were obtained as described previously (Oliveira et al., 2017). Briefly, bone marrow cells were harvested from the tibias and femurs of male and female 6-week-old C57BL/6 mice and cultured independently in BMDM differentiation medium (RPMI supplemented with 30% L929 growth-conditioning media, 20% fetal bovine serum [Gibco], 2-mM glutamine [Sigma-Aldrich], 100 units per millilitre of penicillin–streptomycin [Life Technologies], 50 μM of 2-mercaptoethanol) for 1 week. Fresh media were added every 48 hr. Prior to the tests, cell suspensions were stained with FITC-anti-CD11b (BD Pharmingen, M1/70) and PE-anti-F4/80 (eBioscience, BM8) and analysed by flow cytometry on a FACSCantoII (Becton Dickinson, San Diego, CA) to confirm the macrophage phenotype. Then, 1×10^6 cells were plated into six-well plates for RNA and protein extraction; 2×10^5 BMDMs were plated in 24-well plates to determine phagocytosis and cytotoxicity, and they were also plated into 96-well plates for detection of ROS. All cells were incubated overnight in BMDM experiment medium (BMDM differentiation media with 5% L929 growth-conditioning media and 10% fetal bovine serum) at 37°C under 5% CO_2. For all subsequent experiments, cells were infected at a 1:5 (yeast: BMDM) ratio.

4.8 | Real-time polymerase chain reaction

Total RNA was obtained from adherent BMDMs using TRIzol reagent (Life Technologies, ThermoFisher Scientific, MA, USA) according to the manufacturer's instructions. One microgram of total RNA was used to synthesise the first strand of cDNA, prepared with M-MLV reverse transcriptase (Invitrogen, ThermoFisher Scientific, MA, USA). Quantitative polymerase chain reaction was performed using iTaq™ Universal SYBR® Green Supermix (Bio-Rad) in the CFX96 Touch™ Real-Time detection system (Bio-Rad) to analyse the gene expression of E2 receptors (*Er-alpha*, *Er-beta*, and *Gper*) on non-infected female BMDMs, as well as TLRs (*Tlr2* and *Tlr4*) and dectin-1 fungal receptor on male and female infected BMDMs. *Rpl32* was used as the reference gene in the real-time polymerase chain reaction analyses. The primer sequences used (sense and antisense), from 5′ to 3′, were as follows: *Er-alpha* (TAAGAACCGGAGGAAGAGTTG; TCATGCG GAATCGACTTG-3), *Er-beta* (AAGGTTAGTGGGAACCGTTG; ACAT CCTTCACACGACCAGA), *Gper* (TCCTGCCTCTACACCATCTT; ACA-GGTCTGGGATAGTCATCTT), *Tlr2* (GTGGTACCTGAGAATGATGTG GG; GTTAATTAAGTCAGGAACTGGGTG), *Tlr4* (CTGGGTGAGAAAT GAGCTGG; GATACAATTCCACCTGCTGCC), *dectin-1* (GAACCACA AGCCCACAGAAT; CATGGCCCTTCACTCTGATT), and *Rpl32* (GCT GCCATCTGTTTTACGG; TGACTGGTGCCTGATGAACT). Results are presented as mRNA levels calculated as $2^{-\Delta Ct}$ (where ΔCt is the difference between the Ct of the target gene and that of the *Rpl32* reference gene) and are representative of two independent experiments with three technical replicates.

4.9 | ER modulation

To evaluate the role of the different E2 receptors, BMDMs were first treated for 30 min with an ER-α antagonist (TPBM, 10 nmol L^{-1},

Sigma-Aldrich; Mao et al., 2008), GPER antagonist (G15 or G36, 10 nmol L^{-1}, Phoenix Pharmaceuticals, Inc., Burlingame, CA; Dennis et al., 2011), or GPER agonist (G1, 10 nmol L^{-1}, Cayman Chemical, Ann Arbor, MI) for 30 min (Dennis et al., 2011). Then, they were treated with E2 (10 nmol L^{-1}, Sigma-Aldrich) for 30 min and then infected with Cg. The maximum BMDMs assay time was 24 hr (latest time of infection), with drug replacement every 12 hr.

4.10 | Phagocytosis and killing assays

The phagocytic index (PI) and killing were determined after 2 and 24 hr of infection of BMDM with Cg. Briefly, for PI analyses, cells were plated and infected, as described above, on glass coverslips on the bottom of 24-well plates. After 2 and 24 hr of infection, the glass coverslips were removed and stained with Panótico Rápido dye (Laborclin, Brazil). The PI was expressed as the percentage of BMDM with internalised Cg. For the cytotoxicity assay, in 24-well plates containing infected macrophages, 2 and 24 hr post infection, supernatants were removed, and non-internalised and adherent yeast cells were removed by two washes with PBS. BMDMs were then lysed with 200 μl of sterile distilled water for 30 min at 37°C. Fifty microlitres of diluted lysates were plated onto SDA and incubated for 48 hr at 37°C to determine the intracellular fungal burden (Nicola & Casadevall, 2012). Both phagocytosis and killing assays were performed in six technical replicates, and the data presented are representative of three independent experiments.

4.11 | ROS production

BMDMs were cultured in RPMI1640 without phenol red (Sigma-Aldrich), treated or not with 10-nM E2, infected with Cg, and incubated with 10-μM 2′,7′-dichlorofluorescein diacetate (Invitrogen, Life Technologies, Carlsbad, CA, USA) for ROS quantification. Two and 24 hr post inoculation, fluorescence was assessed by using a fluorometer (Synergy 2 SL Luminescence Microplate Reader; Biotek) using excitation and emission wavelengths of 500 nm. Data are expressed as the mean of arbitrary units of fluorescence of six technical replicates (Ferreira et al., 2013) and are representative of three independent experiments.

4.12 | Western blot

Male and female BMDM proteins were isolated after BMDM Cg infection and from non-infected macrophages. In addition, female BMDM were exposed to 10 nmol L^{-1} of GPER agonist (G1) or 10 nmol L^{-1} of its antagonists (G15 and G36) and then treated with 10 nmol L^{-1} of E2. For each treatment, a non-infected control was performed. After 3 hr of infection, cells were washed twice in PBS and suspended in cell lysis buffer (pH 8.0, 50 mmol L^{-1} of Tris-Base, 100 mmol L^{-1} of NaCl, 5 mmol L^{-1} of EGTA, 50 mmol L^{-1} of $Na_4P_2O_7$, 1 M of MgCl2, 1% Nonidet P/40, 0.3% Triton X-100, 0.5% sodium deoxycholate, and 1% protease inhibitor cocktail; catalogue no. P8340, Sigma-Aldrich). Proteins were quantified by the Bradford method (Bradford, 1976). A protein amount of 30 μg was resolved by SDS-PAGE and transferred to polyvinylidene difluoride membranes, which were probed with anti-phospho-Akt Ser473 (1:1,000; catalogue no. ab109870; Abcam), anti-phospho-PI3K (catalogue no. #4228, 1:1,000; Cell Signaling Technology, Danvers, MA), anti-gp91 (NADPH; catalogue no. sc-74514, 1:1,000; Santa Cruz Biotechnology, Texas, USA), and anticatalase (catalogue no. sc-271803, 1:1,000; Santa Cruz Biotechnology, Texas, USA). Pixel density was normalised to total protein expression using the following antibodies: anti-Akt (1:1,000; catalogue no. ab126811; Abcam) and anti-PI3K (1:1,000, catalogue no. 4292; Cell Signaling Technology, Danvers, MA). Other protein targets were normalised to the reference gene glyceraldehyde 3-phosphate dehydrogenase (GAPDH; 1:1,000, catalogue no. 97166; Cell Signaling Technology). Proteins were detected by using an enhanced chemiluminescence substrate (Amersham Biosciences, Little Chalfont, UK), and the expression levels were expressed as a ratio of optical densities of three biological replicates from three different BMDM cultures.

4.13 | Cryptococcus morphology and Zeta Potential

Cg was grown in Sabouraud Dextrose Broth (SDB) supplemented with E2 (10 nM) under agitation for 48 hr at 37°C. Control Cg was grown in SDB without E2. Cg cells were obtained by centrifugation, suspended in Indian ink, and visualised with an optical microscope (Axioplan; Carl Zeiss). Capsule size and total cell diameter size (diameter plus capsule) of at least 100 cells were measured with ImageJ 1.40 *g* software (National Institutes of Health, Bethesda, MD) and expressed in micrometres. The zeta potential (ZP; ζ) of the yeast cells was calculated by using a ZP analyser (Zetasizer NanoZS90; Malvern, United Kingdom). Cell suspensions in 0.9% NaCl at 600 nm (OD600) were transferred to a cuvette (Cell-Folded Capillary DTS1060; Malvern Instruments), and the ZP was determined at 25°C. The assays for determining ZP were conducted at 25°C using a Zetasizer NanoZS instrument with 64 channels and a correlator at 633 nm (Ferreira et al., 2015; Nosanchuk, Cleare, Franzot, & Casadevall, 1999). Data were expressed as mV ± standard error of two independent experiments.

4.14 | Antifungal drug susceptibility testing

The influence of E2 on the minimum inhibitory concentrations (MICs) of Amphotericin B (AmB) and hydrogen peroxide (HP) against Cg was determined by the antifungal microdilution susceptibility standard test proposed in the CLSI M27-A3 method. AmB was dissolved in 100% DMSO at 1,000 μg ml^{-1}. Both AMB and HP were further diluted in RPMI-1640 (Sigma-Aldrich) to final concentrations ranging from 0.03

to 16 μg ml^{-1} and 4.26 to 272 μg ml^{-1}, respectively. Cg was grown in SDB supplemented with E2 (10 nM) under agitation for 48 hr at 37°C. Control Cg was grown in SDB without E2. The inoculum was prepared in sterile saline to achieve $1.0 \times 10^3 - 5.0 \times 10^3$ cfu ml^{-1}. A 100-μl volume of the inoculum of *Cg* suspension was transferred to sterile flat-bottomed 96-well plates containing 100 μl of each of the antifungals or RPMI-1640 (growth control). The plates were incubated at 35°C for 72 hr. The MICs were determined visually as 100% growth inhibition when compared with the control. All tests were performed in duplicate for each treatment and tested concentration and repeated twice.

4.15 | Lipid peroxidation

Cg was grown in SDB supplemented with E2 (10 nM) under agitation for 48 hr at 37°C. Control Cg was grown in SDB without E2 and treated or not with the MIC of HP for 24 hr at 35°C. The cells were washed with sterile distilled water, and the net wet weight of the pellet was determined. Twenty milligrams of the fungal cell mass of each test was transferred to polypropylene tubes. The products of lipid peroxidation were measured as thiobarbituric acid-reactive substances (TBARSs). The pellet was frozen and homogenised in 1,000-μl ice-cold 1.1% phosphoric acid. The homogenate (400 μl) was mixed with 400 μl of 1% thiobarbituric acid (Sigma-Aldrich) prepared in 50-mM NaOH containing 0.1 mM of butylated hydroxytoluene and 200 μl of 7% phosphoric acid (all the solutions were kept on ice during manipulation). Subsequently, samples (pH 1.5) were heated for 60 min at 98°C, and 1,500 μl of butanol was added. The organic layer was transferred, and the absorbance at 532 nm was measured (Thermo Scientific Multiskan Spectrum, Thermo Fisher Scientific). The thiobarbituric acid solution was replaced with 3 mM of HCl in the blank controls. The TBARS values were expressed using the molar extinction coefficient of 156 mM^{-1} cm^{-1}. The results represent the means of two independent experiments.

4.16 | Antioxidant activity

Prior to the tests, a cell-free extract from 20.0 mg (wet weight) of cells grown in SDB supplemented or not with 10 nM of E2 (35°C for 72 hr) and treated or not with the MIC of hydrogen peroxide for 24 hr at 35°C was prepared according to the method described by Ferreira et al. (2013). Untreated cells were used as controls. These cells were centrifuged and suspended in 2 ml of grinding medium (250-mM sucrose/10-mM Tris–HCl, pH 7.5/1-mM PMSF) and 100 mg of glass beads (0.45 mm). The suspension was disrupted mechanically in a vortex mixer for five cycles of 270 s each of 10,000 vibrations per minute. The homogenate was collected and centrifuged at 1,000 *g* for 5 min at 4°C to remove unbroken cells and glass beads and further centrifuged at 15,000 *g* for 40 min at 4°C. The supernatant was used as a cell-free extract. Soluble protein was determined by using the biuret test and a standard curve of BSA.

The superoxide dismutase (SOD) activity was measured according to the inhibition of pyrogallol autoxidation. The control was performed as 100 μl of grinding medium plus 100 μl of pyrogallol (20 mM; Sigma-Aldrich) diluted in PBS (pH 8.5). Both solutions were prepared fresh at the time of the assay. In the test samples, 100 μl of cell-free extract was added to pyrogallol, and the inhibition of autoxidation was monitored every 30 s for 3 min at a wavelength of 420 nm. The units of SOD were considered as pyrogallol autoxidation per 200 μl and calculated according to Ferreira et al. (2013). The results are expressed in units per milligram of protein and represent the means of three independent experiments.

The peroxidase (PER) activity was measured in a system containing hydrogen peroxide and guaiacol as substrate. The absorbance changes at λ = 470 nm were monitored by using a molar extinction coefficient value of 26.61 M^{-1} cm^{-1} for the product tetraguaiacol formed by the enzymatic reaction. Briefly, 100 μl of the cell-free extract was incubated for 13 min in HEPES solution (25 mM, pH 6.8) containing 10-mM hydrogen peroxide and 4-mM guaiacol (Sigma-Aldrich). The change in absorbance caused by the formation of tetraguaiacol at 470 nm was monitored every 30 s for 3 min of reaction. The lowest absorbance measured was 0.001, and one enzyme unit is the amount of enzyme that produces 1 nmol min^{-1} of product. The results are expressed in nmol min^{-1}/mg^{-1} of protein and represent the means of three independent experiments.

4.17 | Statistical analysis

Results are shown as means ± *SD*. All statistical analyses were performed by using GraphPad Prism, version 5.00, for Windows (GraphPad Software, San Diego, CA, USA), and results were considered significant at $p < .05$. Kaplan–Meier survival curves were generated and analysed using the log-rank test. Western blot analysis, phagocytosis, IPR assay, ROS, and PRN measurements were analysed by analysis of variance, followed by a Tukey test to compare different groups. The results of CFU per gram, capsule size, ZP, and chemokine levels were analysed by the nonparametric Friedman test and used to compare two groups.

ACKNOWLEDGMENT

This study was supported by Fundação de Amparo a Pesquisa do Estado de Minas Gerais-FAPEMIG (Grants APQ-00727-16 and PPM-00061-18), Conselho Nacional de Desenvolvimento Científico e Tecnológico-CNPq and Brazilian Ministry of Healthy (Grants 403006/2016-3 and 440010/2018-7). DAS is a research fellow of the CNPq (Grant 302670/2017-3).

CONFLICT OF INTEREST

The authors declare no potential conflict of interest.

ORCID

Daniel A. Santos https://orcid.org/0000-0002-1108-5666

REFERENCES

Alanio, A., Desnos-Ollivier, M., & Dromer, F. (2011). Dynamics of *Cryptococcus neoformans*-macrophage interactions reveal that fungal background influences outcome during cryptococcal meningoencephalitis in humans. *MBio*, *2*(4), 1–10. https://doi.org/10.1128/mBio.00158-11

Blakemore, J., & Naftolin, F. (2016). Aromatase: Contributions to physiology and disease in women and men. *Physiology (Bethesda)*, *31*(4), 258–269. https://doi.org/10.1152/physiol.00054.2015

Bradford, M. M. (1976). A rapid and sensitive method for the quantitation of microgram quantities of protein utilizing the principle of protein-dye binding. *Analytical Biochemistry*, *72*, 248–254 doi: S0003269776699996 [pii].

Campesi, I., Marino, M., Montella, A., Pais, S., & Franconi, F. (2017). Sex differences in estrogen receptor α and β levels and activation status in LPS-stimulated human macrophages. *Journal of Cellular Physiology*, *232*(2), 340–345. https://doi.org/10.1002/jcp.25425

Charlier, C., Dromer, F., Lévêque, C., Chartier, L., Cordoliani, Y. S., Fontanet, A., … Group, F. C. S. (2008). Cryptococcal neuroradiological lesions correlate with severity during cryptococcal meningoencephalitis in HIV-positive patients in the HAART era. *PLoS One*, *3*(4), e1950. https://doi.org/10.1371/journal.pone.0001950

Clemons, K. V., Shankar, J., & Stevens, D. A. (2016). Mycologic endocrinology. *Advances in Experimental Medicine and Biology*, *874*, 337–363. https://doi.org/10.1007/978-3-319-20215-0_16

Costa, M. C., Santos, J. R., Ribeiro, M. J., Freitas, G. J., Bastos, R. W., Ferreira, G. F., … Santos, D. A. (2016). The absence of microbiota delays the inflammatory response to *Cryptococcus gattii*. *International Journal of Medical Microbiology*, *306*(4), 187–195. https://doi.org/10.1016/j.ijmm.2016.03.010

Dennis, M. K., Field, A. S., Burai, R., Ramesh, C., Petrie, W. K., Bologa, C. G., … Prossnitz, E. R. (2011). Identification of a GPER/GPR30 antagonist with improved estrogen receptor counterselectivity. *The Journal of Steroid Biochemistry and Molecular Biology*, *127*(3–5), 358–366. https://doi.org/10.1016/j.jsbmb.2011.07.002

Ferreira, G. F., Baltazar, L. e. M., Santos, J. R., Monteiro, A. S., Fraga, L. A., Resende-Stoianoff, M. A., & Santos, D. A. (2013). The role of oxidative and nitrosative bursts caused by azoles and amphotericin B against the fungal pathogen *Cryptococcus gattii*. *The Journal of Antimicrobial Chemotherapy*, *68*(8), 1801–1811. https://doi.org/10.1093/jac/dkt114

Ferreira, G. F., Santos, J. R., Costa, M. C., Holanda, R. A., Denadai, Â., Freitas, G. J., … Santos, D. A. (2015). Heteroresistance to itraconazole alters the morphology and increases the virulence of *Cryptococcus gattii*. *Antimicrobial Agents and Chemotherapy*, *59*(8), 4600–4609. https://doi.org/10.1128/AAC.00466-15

Fidel, P. L., Cutright, J., & Steele, C. (2000). Effects of reproductive hormones on experimental vaginal candidiasis. *Infection and Immunity*, *68*(2), 651–657.

Finan, B., Yang, B., Ottaway, N., Stemmer, K., Müller, T. D., Yi, C. X., … Tschöp, M. H. (2012). Targeted estrogen delivery reverses the metabolic syndrome. *Nature Medicine*, *18*(12), 1847–1856. https://doi.org/10.1038/nm.3009

Firacative, C., Lizarazo, J., Illnait-Zaragozí, M. T., Castañeda, E., & Latin American Cryptococcal Study Group. (2018). The status of cryptococcosis in Latin America. *Memórias Do Instituto Oswaldo Cruz*, *113*(7), e170554. https://doi.org/10.1590/0074-02760170554

García-Rodas, R., Casadevall, A., Rodríguez-Tudela, J. L., Cuenca-Estrella, M., & Zaragoza, O. (2011). *Cryptococcus neoformans* capsular enlargement and cellular gigantism during *Galleria mellonella* infection. *PLoS One*, *6*(9), e24485. https://doi.org/10.1371/journal.pone.0024485

Guess, T. E., Rosen, J., Castro-Lopez, N., Wormley, F. L., & McClelland, E. E. (2019). An inherent T-cell deficit in healthy males to *C. neoformans* infection may begin to explain the sex susceptibility in incidence of cryptococcosis. *Biology of Sex Differences*, *10*(1), 44. https://doi.org/10.1186/s13293-019-0258-2

Hurtado, J. C., Castillo, P., Fernandes, F., Navarro, M., Lovane, L., Casas, I., … Martínez, M. J. (2019). Mortality due to *Cryptococcus neoformans* and *Cryptococcus gattii* in low-income settings: An autopsy study. *Scientific Reports*, *9*(1), 7493. https://doi.org/10.1038/s41598-019-43941-w

Jang, B. C., Paik, J. H., Kim, S. P., Bae, J. H., Mun, K. C., Song, D. K., … Suh, S. I. (2004). Catalase induces the expression of inducible nitric oxide synthase through activation of NF-kappaB and PI3K signaling pathway in raw 264.7 cells. *Biochemical Pharmacology*, *68*(11), 2167–2176. https://doi.org/10.1016/j.bcp.2004.08.008

Jimenez, C., Hernandez, C., Pimentel, B., & Carrera, A. C. (2002). The p85 regulatory subunit controls sequential activation of phosphoinositide 3-kinase by Tyr kinases and Ras. *The Journal of Biological Chemistry*, *277*(44), 41556–41562. https://doi.org/10.1074/jbc.M205893200

Kovats, S. (2015). Estrogen receptors regulate innate immune cells and signaling pathways. *Cellular Immunology*, *294*(2), 63–69. https://doi.org/10.1016/j.cellimm.2015.01.018

Leopold Wager, C. M., Hole, C. R., Wozniak, K. L., & Wormley, F. L. (2016). Cryptococcus and phagocytes: Complex interactions that influence disease outcome. *Frontiers in Microbiology*, *7*, 105. https://doi.org/10.3389/fmicb.2016.00105

Levin-Allerhand, J. A., Sokol, K., & Smith, J. D. (2003). Safe and effective method for chronic 17-β-estradiol administration to mice. *Journal of the American Association for Laboratory Animal Science*, *42*(3), 33–35.

Lortholary, O., Improvisi, L., Fitting, C., Cavaillon, J. M., & Dromer, F. (2002). Influence of gender and age on course of infection and cytokine responses in mice with disseminated *Cryptococcus neoformans* infection. *Clinical Microbiology and Infection*, *8*(1), 31–37 doi:375 [pii].

Mao, C., Patterson, N. M., Cherian, M. T., Aninye, I. O., Zhang, C., Montoya, J. B., … Shapiro, D. J. (2008). A new small molecule inhibitor of estrogen receptor alpha binding to estrogen response elements blocks estrogen-dependent growth of cancer cells. *The Journal of Biological Chemistry*, *283*(19), 12819–12830. https://doi.org/10.1074/jbc.M709936200

Mora, D. J., Fortunato, L. R., Andrade-Silva, L. E., Ferreira-Paim, K., Rocha, I. H., Vasconcelos, R. R., … Silva-Vergara, M. L. (2015). Cytokine profiles at admission can be related to outcome in AIDS patients with cryptococcal meningitis. *PLoS One*, *10*(3), e0120297. https://doi.org/10.1371/journal.pone.0120297

McClelland, E. E., Hobbs, L. M., Rivera, J., Casadevall, A., Potts, W. K., Smith, J. M., & Ory, J. J. (2013). The role of host gender in the pathogenesis of *Cryptococcus neoformans* infections. *PLoS One*, *8*(5), e63632. https://doi.org/10.1371/journal.pone.0063632

Mohr, J. A., Tatem, B. A., Long, H., Muchmore, H. G., & Felton, F. G. (1973). Increased susceptibility of *Cryptococcus neoformans* to amphotericin B in the presence of steroids. *Sabouraudia*, *11*(2), 140–142.

Nicola, A. M., & Casadevall, A. (2012). In vitro measurement of phagocytosis and killing of *Cryptococcus neoformans* by macrophages. *Methods in Molecular Biology*, *844*, 189–197. https://doi.org/10.1007/978-1-61779-527-5_14

Nosanchuk, J. D., Cleare, W., Franzot, S. P., & Casadevall, A. (1999). Amphotericin B and fluconazole affect cellular charge, macrophage phagocytosis, and cellular morphology of *Cryptococcus neoformans* at subinhibitory concentrations. *Antimicrobial Agents and Chemotherapy*, *43*(2), 233–239.

Oliveira, L. V. N., Costa, M. C., Magalhães, T. F. F., Bastos, R. W., Santos, P. C., Carneiro, H. C. S., … Santos, D. A. (2017). Influenza a virus as a predisposing factor for Cryptococcosis. *Frontiers in Cellular and Infection Microbiology*, *7*, 419. https://doi.org/10.3389/fcimb.2017.00419

Osterholzer, J. J., Milam, J. E., Chen, G. H., Toews, G. B., Huffnagle, G. B., & Olszewski, M. A. (2009). Role of dendritic cells and alveolar macrophages in regulating early host defense against

pulmonary infection with *Cryptococcus neoformans*. *Infection and Immunity*, *77*(9), 3749–3758. https://doi.org/10.1128/IAI.00454-09

Pacold, M. E., Suire, S., Perisic, O., Lara-Gonzalez, S., Davis, C. T., Walker, E. H., … Williams, R. L. (2000). Crystal structure and functional analysis of Ras binding to its effector phosphoinositide 3-kinase gamma. *Cell*, *103*(6), 931–943. https://doi.org/10.1016/s0092-8674(00)00196-3

Pechous, R. D. (2017). With friends like these: The complex role of neutrophils in the progression of severe pneumonia. *Frontiers in Cellular and Infection Microbiology*, *7*, 160. https://doi.org/10.3389/fcimb.2017.00160

Pennell, L. M., Galligan, C. L., & Fish, E. N. (2012). Sex affects immunity. *Journal of Autoimmunity*, *38*(2–3), J282–J291. https://doi.org/10.1016/j.jaut.2011.11.013

Pinzan, C. F., Ruas, L. P., Casabona-Fortunato, A. S., Carvalho, F. C., & Roque-Barreira, M. C. (2010). Immunological basis for the gender differences in murine *Paracoccidioides brasiliensis* infection. *PLoS One*, *5*(5), e10757. https://doi.org/10.1371/journal.pone.0010757

Pupo, M., Maggiolini, M., & Musti, A. M. (2016). GPER mediates non-genomic effects of estrogen. *Methods in Molecular Biology*, *1366*, 471–488. https://doi.org/10.1007/978-1-4939-3127-9_37

Quinn, M. T., & Gauss, K. A. (2004). Structure and regulation of the neutrophil respiratory burst oxidase: Comparison with nonphagocyte oxidases. *Journal of Leukocyte Biology*, *76*(4), 760–781. https://doi.org/10.1189/jlb.0404216

Rajasingham, R., Smith, R. M., Park, B. J., Jarvis, J. N., Govender, N. P., Chiller, T. M., … Boulware, D. R. (2017). Global burden of disease of HIV-associated cryptococcal meningitis: An updated analysis. *The Lancet Infectious Diseases*, *17*, 873–881. https://doi.org/10.1016/S1473-3099(17)30243-8

Rocha, J. D., Nascimento, M. T., Decote-Ricardo, D., Côrte-Real, S., Morrot, A., Heise, N., … Freire-de-Lima, C. G. (2015). Capsular polysaccharides from *Cryptococcus neoformans* modulate production of neutrophil extracellular traps (NETs) by human neutrophils. *Scientific Reports*, *5*, 8008. https://doi.org/10.1038/srep08008

Santiago-Tirado, F. H., Onken, M. D., Cooper, J. A., Klein, R. S., & Doering, T. L. (2017). Trojan Horse Transit Contributes to Blood-Brain Barrier Crossing of a Eukaryotic Pathogen. *MBio*, *8*(1). https://doi.org/10.1128/mBio.02183-16

Santos, J. R., Holanda, R. A., Frases, S., Bravim, M., Araujo, G. S., Santos, P. C., … Santos, D. A. (2014). Fluconazole alters the polysaccharide capsule of *Cryptococcus gattii* and leads to distinct behaviors in murine Cryptococcosis. *PLoS One*, *9*(11), e112669. https://doi.org/10.1371/journal.pone.0112669

Shaheen, A. A., Somayaji, R., Myers, R., & Mody, C. H. (2018). Epidemiology and trends of cryptococcosis in the United States from 2000 to 2007: A population-based study. *International Journal of STD & AIDS*, *29*(5), 453–460. https://doi.org/10.1177/0956462417732649

Shankar, J., Restrepo, A., Clemons, K. V., & Stevens, D. A. (2011). Hormones and the resistance of women to paracoccidioidomycosis. *Clinical Microbiology Reviews*, *24*(2), 296–313. https://doi.org/10.1128/CMR.00062-10

Sun, D., & Shi, M. (2016). Neutrophil swarming toward *Cryptococcus neoformans* is mediated by complement and leukotriene B4. *Biochemical and Biophysical Research Communications*, *477*(4), 945–951. https://doi.org/10.1016/j.bbrc.2016.07.005

Sun, D., Zhang, M., Liu, G., Wu, H., Li, C., Zhou, H., … Shi, M. (2016). Intravascular clearance of disseminating *Cryptococcus neoformans* in the brain can be improved by enhancing neutrophil recruitment in mice. *European Journal of Immunology*, *46*(7), 1704–1714. https://doi.org/10.1002/eji.201546239

Tica, A. A., Tica, O. S., Georgescu, C. V., Pirici, D., Bogdan, M., Ciurea, T., … Ciurea, M. E. (2016). GPER and ER-α expression in abnormal endometrial proliferations. *Romanian Journal of Morphology and Embryology*, *57*(2), 413–418.

Zaragoza, O., Chrisman, C. J., Castelli, M. V., Frases, S., Cuenca-Estrella, M., Rodríguez-Tudela, J. L., & Casadevall, A. (2008). Capsule enlargement in *Cryptococcus neoformans* confers resistance to oxidative stress suggesting a mechanism for intracellular survival. *Cellular Microbiology*, *10*(10), 2043–2057. https://doi.org/10.1111/j.1462-5822.2008.01186.x

Zhao, H., Tian, Z., Hao, J., & Chen, B. (2005). Extragonadal aromatization increases with time after ovariectomy in rats. *Reproductive Biology and Endocrinology*, *3*, 6. https://doi.org/10.1186/1477-7827-3-6

SUPPORTING INFORMATION

Additional supporting information may be found online in the Supporting Information section at the end of this article.

How to cite this article: Costa MC, de Barros Fernandes H, Gonçalves GKN, et al. 17-β-Estradiol increases macrophage activity through activation of the G-protein-coupled estrogen receptor and improves the response of female mice to *Cryptococcus gattii*. *Cellular Microbiology*. 2020;22:e13179. https://doi.org/10.1111/cmi.13179